

Synthesis, Structure, Luminescence, and Theoretical Studies of Tetranuclear Gold Clusters with Phosphinocarborane Ligands

M. José Calhorda,[†] Olga Crespo,^{‡,§} M. Concepción Gimeno,[‡] Peter G. Jones,^{||} Antonio Laguna,^{*,‡} José M. López-de-Luzuriaga,[⊥] Juan L. Perez,[§] Miguel A. Ramón,[§] and Luís F. Veiros[#]

ITQB, Quinta do Marqués, EAN, Apart. 127, 2781-901, Oeiras, and Departamento de Química e Bioquímica, Faculdade de Ciências, Universidade de Lisboa, 1749-016 Lisboa, Portugal, Departamento de Química Inorgánica, Instituto de Ciencia de Materiales de Aragón, Universidad de Zaragoza-CSIC, E-50009 Zaragoza, Spain, Escuela Universitaria Politécnica de Huesca, Carretera de Cuarte s/n E-22071 Huesca, Spain, Institut für Anorganische und Analytische Chemie der Technischen Universität, Postfach 3329, D-38023 Braunschweig, Germany, Departamento de Química, Universidad de la Rioja, Obispo Bustamante 3, E-26001 Logroño, Spain, and Centro de Química Estrutural, Instituto Superior Técnico, Av. Rovisco Pais, 1096 Lisboa Codex, Portugal

Received February 8, 2000

Treatment of the tetranuclear gold cluster $[\text{Au}_4\{(\text{PPh}_2)_2\text{C}_2\text{B}_9\text{H}_{10}\}_2(\text{AsPh}_3)_2]$ (**1**), which contains the *nido*-carborane-diphosphine $[\text{Au}_4\{(\text{PPh}_2)_2\text{C}_2\text{B}_9\text{H}_{10}\}]^-$, with various tertiary phosphines leads to derivatives $[\text{Au}_4\{(\text{PPh}_2)_2\text{C}_2\text{B}_9\text{H}_{10}\}_2(\text{PR}_3)_2]$ ($\text{PR}_3 = \text{PPh}_3$ (**2**), $\text{P}(4\text{-MeC}_6\text{H}_4)_3$ (**3**), $\text{P}(4\text{-OMeC}_6\text{H}_4)_3$ (**4**)). The X-ray crystal structure of complex **4** shows a tetrahedral framework of gold atoms, two of which are chelated by the diphosphine, and two are coordinated to one monophosphine ligand each. These compounds are very stable and are obtained in high yield. MP2 calculations suggest that the two types of chemically nonequivalent gold atoms can be formally assigned as Au(I) (those attached to the arsines or phosphines) and Au(0) (those bonded to the anionic diphosphine) and emphasize the role of correlation in the gold–gold interactions. The compounds are luminescent. The emission is assigned to a gold-centered spin-forbidden transition; the assignment of the oxidation state of the gold centers on this basis leads to results coincident with those obtained by theoretical calculations.

Introduction

Interest in the chemistry of homo- or heteropolyuclear gold clusters is focused^{1–5} on understanding the formation of such species and thus being in a position to develop a convenient and reproducible synthesis of a given compound. Many well-characterized examples with different nuclearities (4–13 metal atoms) have been described; their nature can be rationalized within a simple metal framework on the basis of Stone's tensor surface harmonic theory.^{6,7} The smallest possible polyhedral gold cluster is tetrahedral Au_4 , for which a particularly stable electronic situation is attained in the dication Au_4^{2+} . The species $[\text{AuL}]_4^{2+}$, with L representing a 3-fold rotor ligand, is expected to adopt full tetrahedral symmetry.⁸ Such small clusters are

poorly represented; the tetrahedral clusters described thus far are $[\text{Au}_4\text{I}_2(\text{PPh}_3)_4]$,⁹ $[\text{Au}_4(\text{SnCl}_3)_2(\text{PPh}_3)_4]$,¹⁰ $[\text{AuL}]_4(\text{BF}_4)_2$ ($\text{L} = \text{P}^t\text{Bu}_3$, $\text{P}(\text{mesityl})_3$).^{11,12} All are minor products (yields 5–15%) with the exception of $[\text{Au}_4\{\text{P}(\text{mesityl})_3\}_4](\text{BF}_4)_2$ and $[\text{Au}_4\{(\text{PPh}_2)_2\text{C}_2\text{B}_9\text{H}_{10}\}_2(\text{AsPh}_3)_2]$;¹³ the latter has been previously communicated by us as part of our studies involving partial degradation of the diphosphine¹⁴ $[\text{1,2-}(\text{PPh}_2)_2\text{C}_2\text{B}_{10}\text{H}_{10}]$ to afford the anionic *nido*-diphosphine ligand $[\text{7,8-}(\text{PPh}_2)_2\text{C}_2\text{B}_9\text{H}_{10}]^-$. Here we report the synthesis of the derivatives $[\text{Au}_4\{(\text{PPh}_2)_2\text{C}_2\text{B}_9\text{H}_{10}\}_2(\text{PR}_3)_2]$ ($\text{PR}_3 = \text{PPh}_3$ (**2**), $\text{P}(4\text{-MeC}_6\text{H}_4)_3$ (**3**), $\text{P}(4\text{-OMeC}_6\text{H}_4)_3$ (**4**)). These compounds are very stable and obtained in high yield. Theoretical and luminescence studies of these tetranuclear complexes and the structural study of **4** by X-ray diffraction have been carried out.

* Author to whom correspondence should be addressed. Telephone: +34-976-761185. Fax: +34-976-761187. E-mail: alaguna@posta.unizar.es.

[†] ITQB, Quinta do Marqués, EAN, and Universidade de Lisboa.

[‡] Universidad de Zaragoza-CSIC.

[§] Escuela Universitaria Politécnica de Huesca.

^{||} Institut für Anorganische und Analytische Chemie der Technischen Universität, Braunschweig.

[⊥] Universidad de la Rioja.

[#] Instituto Superior Técnico, Lisboa.

(1) Hall, K. P.; Mingos, D. M. P. *Prog. Inorg. Chem.* **1984**, *32*, 237.

(2) Mingos, D. M. P.; Watson, M. J. *Transition Met. Chem.* **1991**, *16*, 285.

(3) Teo, B. K.; Zang, S. H. *J. Am. Chem. Soc.* **1992**, *114*, 2743.

(4) Fackler, J. P.; Winpenny, R. E. P.; Pignolet, L. H. *J. Am. Soc.* **1989**, *111*, 6434.

(5) Schmidt, G. *Chem. Rev.* **1992**, *92*, 1709.

(6) Mingos, D. M. P. *Polyhedron* **1984**, *3*, 1289.

(7) Stone, A. J. *Mol. Phys.* **1980**, *41*, 1331.

(8) Mingos, D. M. P. *Gold Bull.* **1984**, *17*, 5.

Discussion

Synthesis. We have previously communicated the synthesis of the tetranuclear gold cluster $[\text{Au}_4\{(\text{PPh}_2)_2\text{C}_2\text{B}_9\text{H}_{10}\}_2(\text{AsPh}_3)_2]$ (**1**) by reaction of the diphosphine $[(\text{PPh}_2)_2\text{C}_2\text{B}_{10}\text{H}_{10}]$ with

(9) Demartin, F.; Manassero, M.; Naldini, L.; Ruggeri, R.; Sansoni, M. *J. Chem. Soc., Chem. Commun.* **1981**, 222.

(10) Mingos, D. M. P.; Powell, H. R.; Stolberg, T. L. *Transition Met. Chem.* **1992**, *17*, 334.

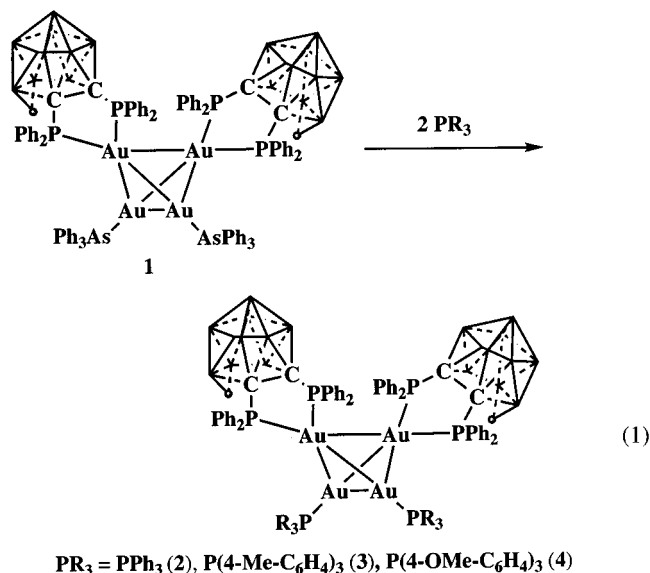
(11) Zeller, E.; Beruda, H.; Schmidbaur, H. *Inorg. Chem.* **1993**, *32*, 3203.

(12) Yang, Y.; Sharp, P. R. *J. Am. Chem. Soc.* **1994**, *116*, 8983.

(13) Crespo, O.; Gimeno, M. C.; Laguna, A.; Jones, P. G.; Villacampa, M. D. *Angew. Chem., Int. Ed. Engl.* **1997**, *36*, 992.

(14) Crespo, O.; Gimeno, M. C.; Laguna, A.; Jones, P. G. *Inorg. Chem.* **1996**, *35*, 1361.

[AuCl(AsPh₃)] in ethanol. Compound **1** is obtained in high yield and can be used as a starting material in substitution reactions of the arsine by phosphine ligands. Thus the reaction of [Au₄{(PPh₂)₂C₂B₉H₁₀}₂(AsPh₃)₂] (**1**) (eq 1) with tertiary phosphines



in a 1:2 molar ratio affords the derivatives [Au₄{(PPh₂)₂C₂B₉H₁₀}₂(PR₃)₂] (PR₃ = PPh₃ (**2**), P(4-MeC₆H₄)₃ (**3**), P(4-OMeC₆H₄)₃ (**4**)). Complexes **2–4** are yellow solids, moisture- and air-stable, which behave as nonconductors in acetone solutions. In their IR spectra the $\nu(\text{B-H})$ frequencies appear at 2587 (**2**), 2585 (**3**), and 2578 cm⁻¹ (**4**); these are lower than those found in complexes with the *closo*-diphosphine, which is characteristic of the partially degraded nature of the ligand. The ¹H NMR spectra show for all the complexes a broad signal at about -2 ppm, which corresponds to the bridging hydrogen atom in the open face of the carborane core. The ³¹P{¹H} spectra of these compounds consist of AA'BB'XX' systems which have been simulated in order to confirm their nature (see Experimental Section). In their positive liquid secondary impact mass spectra (LSIMS) the molecular peaks appear at $m/z = 2316$ (22%) (**2**), 2400 (11%) (**3**), and 2496 (26%) (**4**).

The structure of compound **4** (as the acetone trisolvate) has been studied by X-ray diffraction; the molecule is shown in Figure 1 and consists of a tetrahedral gold core in which two of the gold atoms (Au1 and Au2) are chelated by the anionic diphosphine, and each of the other two is bonded to one tris(*p*-methoxyphenyl)phosphine ligand. The Au-Au distances can be classified into medium (Au(1)-Au(4) 2.8722(3) Å, Au(2)-Au(3) 2.8648(3) Å, Au(3)-Au(4) 2.8608(4) Å) or short (Au(1)-Au(2) 2.6350(3) Å, Au(1)-Au(3) 2.6514(3) Å, Au(2)-Au(4) 2.6291(3) Å). These values are similar to those found in other tetrahedral gold clusters such as [Au₄I₂(PPh₃)₄]⁹ (2.6959(1)-2.828(1) Å) or [Au₄(μ -SnCl₃)₂(PPh₃)₄]¹⁰ (2.6341(5)-2.8228(5) Å). A narrower range of distances was found in [Au₄{P(mesityl)₃}₄]²⁺ (2.7031(9)-2.7302(7) Å),¹² but a wider range (from 2.6036(7) to 2.9148(8) Å) in compound **1** [Au₄{(PPh₂)₂C₂B₉H₁₀}₂(AsPh₃)₂].¹⁴ The shortest of these values are also the shortest distances found in this type of cluster. The Au-P distances corresponding to the diphosphine ligands (2.3590(11)-2.4164(11) Å) are in the range of those found for the precursor **1** (2.342(2)-2.373(2) Å). These distances are longer than those corresponding to the monophosphine ligands (2.2988(11), 2.2977(12) Å), which are in turn similar to the values found in other related clusters with monodentate phos-

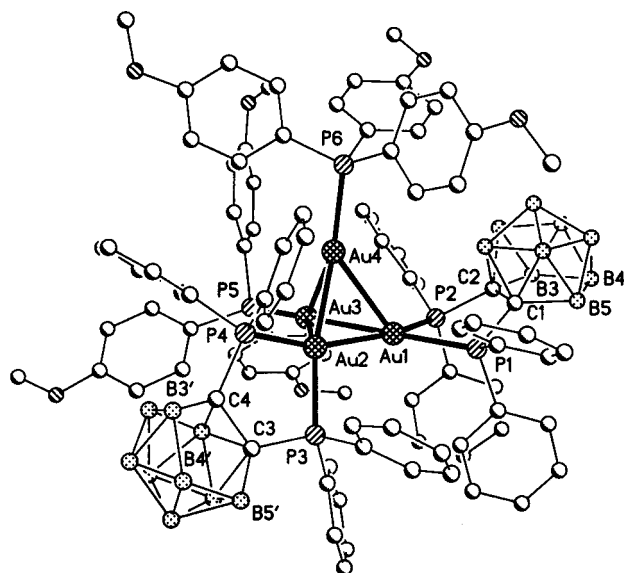


Figure 1. Crystal structure of compound **4** with the atom-numbering scheme. Hydrogens have been omitted for clarity. Radii are arbitrary.

phine ligands such as [Au₄I₂(PPh₃)₄] (2.289(3), 2.292(3) Å) or [Au₄(P^tBu₃)₄]BF₄ (2.304(4)-2.306(4) Å). The coordination geometry at Au1 and Au2 is distorted trigonal bipyramidal, the phosphorus atoms of the diphosphine occupying one equatorial and one axial position. The distortions mainly arise from the restraints of the tetrahedral cluster geometry. The angles P2-Au1-P1 and P3-Au1-P4 (82.73(4)°, 88.17(4)° respectively) are close to ideal, and the angles P2-Au2-Au4 168.18(3)° and P2-Au1-Au2 159.61(3)° approach linearity, although the distortion is more marked than in the similar carborane cluster **1**. A selection of bond angles and lengths is shown in Table 1.

Theoretical Calculations. Theoretical calculations were performed in order to understand the bonding and assign formal oxidation states to gold atoms, as there are two types of nonequivalent gold atoms in these Au₄ clusters. Calculations on the more symmetric (AuL)₄²⁺ (L = phosphine) clusters had been performed before, either at the HF and MP2 level¹⁵ or at the CNDO/1 level including quasi-relativistic or relativistic corrections.¹⁶

While both HF and MP2 were able to reproduce the Au-Au distances reliably, there was a significant energy lowering when the MP2 approach was used, indicating that although the gold-gold bonds have a strong covalent character, correlation is still significant.¹⁵

In view of the size of the [(AuL)₂(AuL')₂]²⁺ (L = EH₃, E = P, As, L' = bidentate phosphine) clusters, exploratory extended Hückel calculations were performed first. This allowed the choice of a good model to be used in the ab initio calculations. The most important requirement of the model was the choice of a relatively rigid bidentate phosphine, which prevented the P-Au-P angle from opening. Indeed, initial geometry optimization calculations where this constraint was not taken into account led to disassembling of the cluster. EH calculations were performed with fixed Au-Au distances (see Experimental Section for details) for the simplest possible model, [(AuH)₂(AuH)₂]⁴⁻ (A), for the more realistic model [(Au(AsH₃))₂{Au(PH₂CH₂CH₂PH₂)₂]²⁺ (B), and for the X-ray-determined structure (C). The charge distribution on the gold atoms showed two atoms to bear more negative charges (Au1

(15) Pyykkö, P.; Runeberg, N. *J. Chem. Soc., Chem. Commun.* **1993**, 1812.

(16) Boca, R. *J. Chem. Soc., Dalton Trans.* **1994**, 2061.

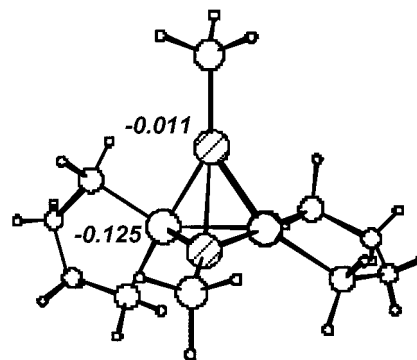
Table 1. Selected Bond Lengths (Å) and Angles (deg) for Compound 4

Au(1)–P(2)	2.3657(11)	Au(4)–P(6)	2.2977(12)
Au(1)–P(1)	2.4164(11)	P(1)–C(21)	1.833(5)
Au(1)–Au(2)	2.6350(3)	P(1)–C(1)	1.837(4)
Au(1)–Au(3)	2.6514(3)	P(1)–C(11)	1.842(3)
Au(1)–Au(4)	2.8722(3)	P(2)–C(2)	1.829(4)
Au(2)–P(3)	2.3590(11)	P(3)–C(3)	1.833(4)
Au(2)–P(4)	2.3636(10)	P(4)–C(4)	1.841(4)
Au(2)–Au(4)	2.6291(3)	C(1)–C(2)	1.599(6)
Au(2)–Au(3)	2.8648(3)	C(3)–C(4)	1.597(6)
Au(3)–P(5)	2.2988(11)	P(3)–C(3)	1.833(4)
Au(3)–Au(4)	2.8608(4)	P(4)–C(4)	1.841(4)
P(2)–Au(1)–P(1)	82.73(4)	Au(1)–Au(3)–Au(2)	56.911(7)
P(2)–Au(1)–Au(2)	159.61(3)	Au(4)–Au(3)–Au(2)	54.669(8)
P(1)–Au(1)–Au(2)	117.60(3)	P(6)–Au(4)–Au(2)	156.52(3)
P(2)–Au(1)–Au(3)	94.02(3)	P(6)–Au(4)–Au(3)	139.04(3)
P(1)–Au(1)–Au(3)	176.70(3)	Au(2)–Au(4)–Au(3)	62.742(6)
Au(2)–Au(1)–Au(3)	65.626(8)	P(6)–Au(4)–Au(1)	137.18(3)
P(2)–Au(1)–Au(4)	116.11(3)	Au(2)–Au(4)–Au(1)	57.032(6)
P(1)–Au(1)–Au(4)	119.76(3)	Au(3)–Au(4)–Au(1)	55.094(8)
Au(2)–Au(1)–Au(4)	56.833(8)	C(21)–P(1)–Au(1)	109.39(14)
Au(3)–Au(1)–Au(4)	62.234(9)	C(1)–P(1)–Au(1)	103.73(14)
P(3)–Au(2)–P(4)	88.17(4)	C(11)–P(1)–Au(1)	123.73(10)
P(3)–Au(2)–Au(4)	168.18(3)	C(31)–P(2)–Au(1)	119.02(13)
P(4)–Au(2)–Au(4)	97.42(3)	C(41)–P(2)–Au(1)	112.37(13)
P(3)–Au(2)–Au(1)	107.17(3)	C(2)–P(2)–Au(1)	105.34(14)
P(4)–Au(2)–Au(1)	162.92(3)	C(61)–P(3)–Au(2)	109.80(14)
Au(4)–Au(2)–Au(1)	66.135(9)	C(51)–P(3)–Au(2)	120.57(13)
P(3)–Au(2)–Au(3)	123.11(3)	C(3)–P(3)–Au(2)	106.32(14)
P(4)–Au(2)–Au(3)	120.39(3)	C(71)–P(4)–Au(2)	119.14(13)
Au(4)–Au(2)–Au(3)	62.590(8)	C(81)–P(4)–Au(2)	112.88(13)
Au(1)–Au(2)–Au(3)	57.463(8)	C(4)–P(4)–Au(2)	106.29(13)
P(5)–Au(3)–Au(1)	161.66(3)	C(111)–P(5)–Au(3)	113.46(14)
P(5)–Au(3)–Au(4)	129.11(3)	C(101)–P(5)–Au(3)	110.50(13)
Au(1)–Au(3)–Au(4)	62.671(7)	C(131)–P(6)–Au(4)	109.74(14)
P(5)–Au(3)–Au(2)	140.24(3)	C(141)–P(6)–Au(4)	110.00(16)

and Au2, see crystal structure for numbering system), respectively -0.327 , -0.294 , and $-0.411/-0.430$ for A, B, and C. At Au3 and Au4 the charges were calculated to be -0.166 , -0.255 , and $-0.254/-0.252$, respectively. This led to an assignment of Au1 and Au2 as being formally Au(0), while Au3 and Au4 were Au(I), preserving the overall charge $2+$ for the cluster core.

HF calculations, under C_2 symmetry, led to relatively long Au–Au distances (four of 2.872 Å, one of 2.911 Å, and another of 2.947 Å). In contrast, the agreement between experimentally observed distances and those calculated with MP2 under the same conditions (four of 2.772, one of 2.754, and another of 2.915 Å) is significantly better. The Au–As distance also decreases from 2.612 Å at the HF level to 2.529 Å at the MP2 level, approaching the observed value of 2.389 Å. The agreement is not as good as that found by Pyykkö et al.,¹⁵ probably owing to the worse quality of the basis set used. The charge distribution (MP2) shows a more negative charge at Au1 and Au2 than at Au3 and Au4 (-0.125 and -0.011 , respectively), as can be seen in Figure 2. The cause of the different electron richness of the two types of gold centers can be traced to the presence of the chelate phosphine, which imposes a rigid P–Au–P angle and determines the shape and energy of the frontier orbitals of Au1 and Au2. If this angle is forced to widen, the situation changes drastically, as these gold atoms become better suited as donors than acceptors. The charge distribution is therefore reversed.

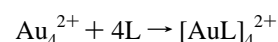
In the symmetrical $[\text{AuPH}_3]_4^{2+}$ cluster (MP2 calculations, same conditions), the charge on each gold atom is 0.048. The Au–Au distance was calculated as 2.806 and 2.901 Å, a value

**Figure 2.** Au–Au formal charges in the model cluster $[\text{Au}_4(\text{AsH}_3)_2(\text{H}_2\text{PCH}_2\text{CH}_2\text{PH}_2)_2]^{2+}$.**Table 2.** Enthalpy Changes (kcal mol^{-1}) for the Formation of the Phosphine (Arsine) Complexes $[\text{AuL}]_4^{2+}$

	HF	MP2
L = PH_3	-7.07	-10.22
L ₄ = $(\text{AsH}_3)_2(\text{H}_2\text{PCH}_2\text{CH}_2\text{PH}_2)_2$	-6.87	-11.39

relatively long compared with the 2.730 Å found experimentally for $[\text{Au}^{\text{I}}\text{Bu}_3]_4^{2+}$.¹¹

We also calculated the enthalpy (ΔE) of the reaction



for $4\text{L} = (\text{PH}_3)_4$ and $(\text{AsH}_3)_2(\text{H}_2\text{PCH}_2\text{CH}_2\text{PH}_2)_2$, using both the HF and the MP2 approach, in order to compare the results for the two types of compounds (Table 2). The low symmetry and large variety of atoms of the present cluster made it impossible for us to use a very good basis set in the calculations.

These values differ significantly from those of the literature (for PH_3),¹⁵ as a result of the smaller basis set used. The effect of correlation on the energy is, however, very similar for the two types of clusters, in spite of the chemical differences between the gold atoms (all equivalent for the PH_3 cluster, of two types for the other) and the resulting differences in bonding.

Luminescence Studies. The study of luminescent gold(I) compounds has received great attention and developed rapidly in the last years. Particularly interesting are multimetallic systems that show metal–metal interactions, because the study of their photophysical and photochemical properties, apart from their fundamental interest, has potential applications in synthesis, energy conversion, and pharmacology.¹⁷

One approach for achieving multiphoton and multielectron reactions is to synthesize cluster complexes where the metal centers are in close communication, but whereas examples of luminescent gold(I) complexes with short $\text{Au}\cdots\text{Au}$ contacts are abundant, to date the literature contains few emitting heteropolynuclear gold-metal clusters¹⁸ and to the best of our knowledge, there have been no reports on the luminescence behavior of gold clusters that exhibit an average formal oxidation state $<+1$.

Complexes **1–4** show an intense luminescence both at room temperature and at 77 K in the solid state. Their excitation spectra show a very complicated profile with maxima at ca. 390 nm, associated with maximum emission bands appearing in the range 640–660 nm at room temperature and at 689–662 nm at 77 K (see Table 3).

The observation that the emission wavelength is different for the four complexes suggests that the luminescence is not an

(17) Yam, V. W. W.; Lo, K. K. W. *Chem. Soc. Rev.* **1999**, 28, 323.(18) Zhang, T.; Drouin, M.; Harvey, P. D. *Inorg. Chem.* **1999**, 38, 4928.

Table 3. Luminescence Data (λ_{max} , nm) for Complexes 1–4

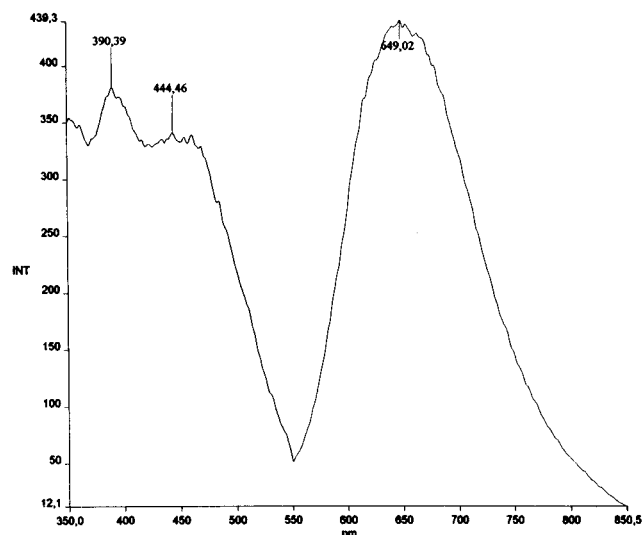
	solid state				chloroform solution: 5×10^{-4} M	
	298 K		77 K		excitation	emission
	excitation	emission	excitation	emission		
1	389	661	389	689	476	685
2	390	649	390	666	480	657
3	391	646	389	666	409	667
4	393	640	391	662	475	662

intraligand transition from a π orbital associated with the carborane ligand, since a change in energy difference would not be anticipated in that case. Also, emissions associated with phenyl rings usually appear at higher energies.¹⁹ Thus, we tentatively assume that the atoms labeled 3 and 4 in the crystal structure are responsible for the luminescence, which are the centers bonded to different ligands in the four complexes and, according to our theoretical results, formally in oxidation state +1.

Taking into account the charge distribution obtained in our theoretical calculations (see above), we can consider the phosphocarborane ligands and the gold centers directly bonded to them, which are in formal oxidation state 0, as the negative moieties bonded to two $[\text{Au-L}]^+$ units and keeping short contacts between the two gold(I) centers (2.86 Å). In such systems a phosphorescent emission originating from a metal-centered (MC) $d_z^2-p_z$ transition is expected.²⁰ Indeed, the large Stokes shift between the excitation and emission bands (> 10000 cm^{-1}) is indicative of a large distortion in the excited state (compared to the ground state) and suggests that the emission is phosphorescence. Besides, in the atomic spectrum of the Au^+ ion, the energy difference between the singlet $^1\text{S}_0$ ground state and the lower triplet state $^3\text{D}_3$ is 15039 cm^{-1} .²¹ In the four compounds emission occurs roughly at this energy (15128 (1), 15408 (2), 15479 (3), and 15625 cm^{-1} (4)) at room temperature.

The red shift observed in the emission bands with increasing temperature is consistent with an increase in the Au–Au separation as a result of thermal expansion. This fact seems to indicate that the gold–gold distances have a significant influence on the HOMO–LUMO gap, which increases with increasing Au–Au distances.

A theoretical study by Pyykkö and co-workers in a model in which two perpendicular $[\text{X-Au-L}]$ units keep short metal–metal interactions ($\text{X} = \text{halogenide}$; $\text{L} = \text{neutral ligand}$) showed that the aurophilic $\text{Au}\cdots\text{Au}$ interactions increase with the softness of the ligands.²² This study was experimentally confirmed by Fackler and Schmidbaur and co-workers in a series of complexes $[\text{X-Au-L}]$ ($\text{X} = \text{Cl, Br, I}$; $\text{L} = \text{TPA, HTPA}$) (TPA = 1,3,5-triaza-7-phosphaadamantane), in which a reduced softness of the P donor ligand upon protonation causes an increase in the gold–gold distance.²³ The consequence is that, as the two metal centers approach, a decrease in the HOMO–LUMO gap for a metal-centered transition and a red shift in

**Figure 3.** Emission and excitation spectra in the solid state at room temperature for compound 2.

the emission energies would be expected.^{23b,24} These results are also in accordance with the emission wavelengths observed in our complexes at different temperatures, because as the softness increases in the series phosphines < arsines, the wavelength is red-shifted in the same order.

Nevertheless, the experimental metal–metal distances found between the formally +1 gold centers are longer for the arsine derivative (2.9148 Å) than the complex 4 with the phosphine $\text{P}(4\text{-OMeC}_6\text{H}_4)_3$ (2.8608 Å), while the remaining distances involving these gold atoms are shorter in the arsine derivative. These facts seem to indicate that the influence of the gold atoms 1 and 2, formally in the 0 oxidation state (see above), cannot be excluded in the transition that gives rise to luminescence. In fact, previous studies carried out on tetranuclear halogenide copper complexes showed bands at similar high energies, which were suggested to originate from a cluster-centered excited state mixed with an LMCT (ligand to metal charge transfer) delocalized over the core.²⁵ Besides, the larger AsPh_3 ligands (compared to phosphines) presumably contribute to the lengthening of the $\text{Au(I)}\cdots\text{Au(I)}$ interaction.

Finally, luminescence studies in 5×10^{-4} M chloroform solutions have also been carried out (see Table 3). Emission wavelengths similar to those obtained for the complexes in the solid state seem to indicate that the structure of compounds 2–4 is the same in chloroform solution and in the solid. Confirmation of this point is also obtained from the $^{31}\text{P}\{^1\text{H}\}$ NMR spectra. (Figures 3–5 show the emission and excitation spectra in the solid state (room temperature and 77 K) and in chloroform solution for compound 2.

Experimental Section

General. IR spectra were recorded in the range 4000 – 200 cm^{-1} on a Perkin-Elmer 883 spectrophotometer using Nujol mulls between polyethylene sheets. Conductivities were measured in ca. 5×10^{-4} mol dm^{-3} solutions with a Philips 9509 conductimeter. C and H analyses were carried out with a Perkin-Elmer 2400 microanalyzer. Mass spectra were recorded on a VG Autospec, with the LSIMS technique, using nitrobenzyl alcohol as matrix. NMR spectra were

(19) Larson, L. J.; McMacaulay, E. M.; Weissbart, B.; Tinti, D. J. *J. Phys. Chem.* **1995**, *99*, 7218.

(20) Forward, J. M.; Fackler, J. P., Jr.; Assefa, Z. In *Optoelectronic Properties of Inorganic Compounds*; Roundhill, D. M., Fackler, J. P., Jr., Eds.; Plenum Press: New York, 1999; pp 195–226.

(21) *Atomic Energy Levels*, circular 467; Moore, C. E., Ed.; U.S. Department of Commerce, National Bureau of Standards: Washington, DC, 1958; Vol. 3, p 190.

(22) Pyykkö, P.; Li, J.; Runeberg, N. *Chem. Phys. Lett.* **1994**, *218*, 133.

(23) (a) Assefa, Z.; McBurnett, B. G.; Staples, R. J.; Fackler, J. P., Jr. *Inorg. Chem.* **1995**, *34*, 4965. (b) Assefa, Z.; McBurnett, B. G.; Staples, R. J.; Fackler, J. P., Jr.; Assmann, B.; Angermaier, K.; Schmidbaur, H. *Inorg. Chem.* **1995**, *34*, 75.

(24) (a) Jaw, H. R. C.; Savas, M. M.; Rodgers, R. D.; Mason, W. R. *Inorg. Chem.* **1989**, *28*, 1028. (b) Che, C. M.; Kwong, H. L.; Poon, C. K.; Yam, V. W. W. *J. Chem. Soc., Dalton Trans.* **1990**, 3215.

(25) (a) Ford, P. C.; Vogler, A. *Acc. Chem. Res.* **1993**, *26*, 220. (b) Ford, P. C. *Coord. Chem. Rev.* **1994**, *132*, 129. (c) Vitale, M.; Palke, W. E.; Ford, P. C. *J. Phys. Chem.* **1992**, *96*, 8329.

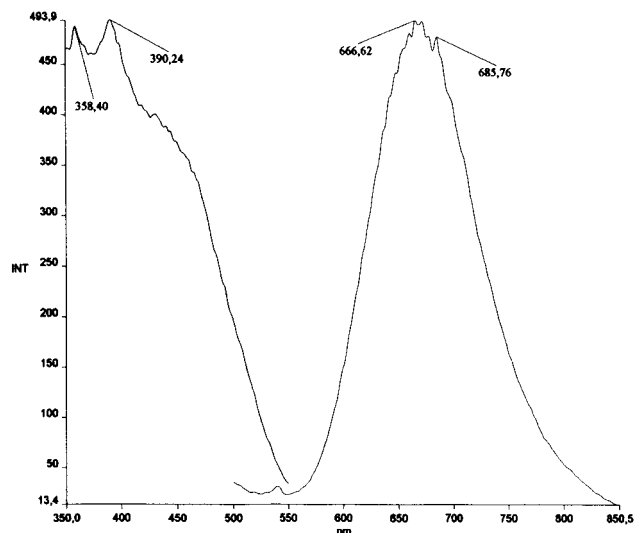


Figure 4. Emission and excitation spectra in the solid state at 77 K for compound **2**.

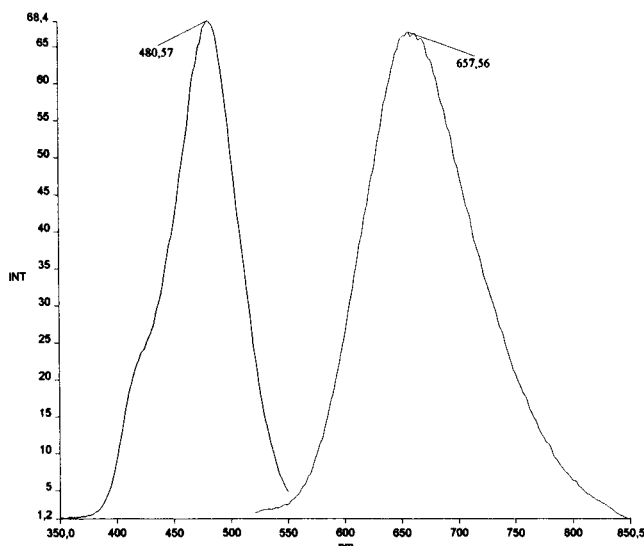


Figure 5. Emission and excitation spectra in chloroform solution (5×10^{-4} M) for compound **2**.

recorded on a Varian Unity 300 spectrometer and a Bruker ARX 300 spectrometer in CDCl_3 . Chemical shifts are cited relative to SiMe_4 (^1H , external) and 85% H_3PO_4 (^{31}P , external). The starting materials $[\text{AuCl}(\text{AsPh}_3)]^{19}$ and $[1,2\text{-}(\text{PPh}_2)_2\text{C}_2\text{B}_{10}\text{H}_{10}]^{20}$ were prepared by literature methods and the phosphines PPh_3 , $\text{P}(4\text{-MeC}_6\text{H}_4)_3$ and $\text{P}(4\text{-OMeC}_6\text{H}_4)_3$ obtained from Aldrich and used as given.

Synthesis of $[\text{Au}_4\{(\text{PPh}_2)_2\text{C}_2\text{B}_9\text{H}_{10}\}_2(\text{PR}_3)_2]$ ($\text{PR}_3 = \text{PPh}_3$ (2**), $\text{P}(4\text{-MeC}_6\text{H}_4)_3$ (**3**), $\text{P}(4\text{-OMeC}_6\text{H}_4)_3$ (**4**)).** To a solution of **1** in dichloromethane (0.240 g, 0.1 mmol) was added PR_3 ($\text{PR}_3 = \text{PPh}_3$ (0.052 g, 0.2 mmol, **2**), $\text{P}(4\text{-MeC}_6\text{H}_4)_3$ (0.061 g, 0.2 mmol, **3**), $\text{P}(4\text{-OMeC}_6\text{H}_4)_3$ (0.070 g 0.2 mmol, **4**)). After stirring for 30 min the solution was concentrated to ca. 5 mL and hexane (10 mL) added. Compounds **2–4** were obtained as yellow solids. **2**: yield 68%. Anal. Found: C, 45.2; H, 4.05. Calcd for $\text{C}_{88}\text{H}_{90}\text{Au}_4\text{B}_{18}\text{P}_6$: C, 45.65; H, 3.9. ^1H NMR: -2 ppm (s, br, 1H, bridging H), 6.2–8 (m, 15H, Ph). $^{31}\text{P}\{^1\text{H}\}$ NMR: AA'BB'XX' system, $\delta_A = \delta_{A'} = 98.3$, $\delta_B = \delta_{B'} = 89.7$, $J_{AA'} = 300$ Hz, $J_{AB} = J_{A'B'} = 50$ Hz, $\delta_X = 51.3$, $\delta_{X'} = 51$, $J_{AX} = J_{AX'} = 200$ Hz, $J_{BX} = J_{B'X'} = 100$ Hz. **3**: yield 74%. Anal. Found: C, 46.65; H, 4.35. Calcd for $\text{C}_{94}\text{H}_{102}\text{Au}_4\text{B}_{18}\text{P}_6$: C, 47.05; H, 4.30. ^1H NMR: -2 ppm (s, br, 1H, bridging H), 2.12 (d, 9H, $J(\text{P-H}) = 18.8$ Hz, Me), 6.2–8.2 (m, 12H, Ph). $^{31}\text{P}\{^1\text{H}\}$ NMR: AA'BB'XX' system, $\delta_A = \delta_{A'} = 95$, $\delta_B = \delta_{B'} = 91$, $J_{AA'} = 190$ Hz, $J_{AB} = J_{A'B'} = 50$ Hz, $\delta_X = \delta_{X'} = 51$, $J_{AX} = J_{AX'} = 190$ Hz, $J_{BX} = J_{B'X'} = 85$ Hz. **4**: yield 63%. Anal. Found: C, 45.25; H, 4.25. Calcd for $\text{C}_{94}\text{H}_{102}\text{Au}_4\text{B}_{18}\text{O}_6\text{P}_6$: C, 45.25; H, 4.10. ^1H

Table 4. Details of Data Collection and Structure Refinement for Complex **4**

chem formula	$\text{C}_{103}\text{H}_{120}\text{Au}_4\text{B}_{18}\text{P}_6$	M	2670.26
cryst habit	orange prism	$F(000)$	2612
cryst size/mm	$0.42 \times 0.20 \times 0.18$	$T/^\circ\text{C}$	-130
cryst syst	triclinic	$2\theta_{\text{max}}/\text{deg}$	60.6
space group	$P(-1)$	$\mu(\text{Mo K}\alpha)/\text{cm}^{-1}$	56
$\lambda/\text{\AA}$	0.71073	transm	0.636–0.163
$a/\text{\AA}$	14.6994(16)	no. of reflns measd	66347
$b/\text{\AA}$	17.947(2)	no. of unique reflns	32403
$c/\text{\AA}$	21.550(2)	R_{int}	0.0705
α/deg	89.328(3)	$R^a (F > 4\sigma(F))$	0.0357
β/deg	81.040(3)	$R_w^b(F^2, \text{all reflns})$	0.0680
γ/deg	72.477(3)	no. of params	1297
$V/\text{\AA}^3$	5351.6(10)	no. of restraints	1298
Z	2	σ^c	0.875
$D_c/\text{g cm}^{-3}$	1.657	max $\Delta\rho/e \text{\AA}^{-3}$	1.751

$^a R(F) = \sum(|F_o| - |F_c|)/\sum|F_o|$. $^b R_w(F^2) = [\sum\{w(F_o^2 - F_c^2)^2\}/\sum\{w(F_o^2)^2\}]^{0.5}$; $w^{-1} = \sigma^2(F_o^2) + (aP)^2 + bP$, where $P = [F_o^2 + 2F_c^2]/3$ and a and b are constants adjusted by the program. $^c S = [\sum\{w(F_o^2 - F_c^2)^2\}/(n - p)]^{0.5}$, where n is the number of data and p the number of parameters.

NMR: -2 ppm (s, br, 1H, bridging H), 3.72 (s, 9H, OMe), 6.2–8 (m, 12 H, Ph). $^{31}\text{P}\{^1\text{H}\}$ NMR: AA'BB'XX' system, $\delta_A = \delta_{A'} = 97.5$, $\delta_B = \delta_{B'} = 88.0$, $J_{AA'} = 300$ Hz, $J_{AB} = J_{A'B'} = 60$, $\delta_X = \delta_{X'} = 47$, $J_{AX} = J_{A'X'} = 260$ Hz, $J_{BX} = J_{B'X'} = 120$ Hz, $J_{XX'} = 7$ Hz.

Crystal Structure Determinations. The crystal was mounted in inert oil on a glass fiber and transferred to the cold gas stream of a Bruker SMART 1000 CCD area detector equipped with an LT-3 low-temperature attachment. Data were collected using monochromated Mo $\text{K}\alpha$ radiation ($\lambda = 0.71073$ \AA), scan type ω . A ΔF -absorption correction was applied with the program SHELXA. The structure was solved by direct methods and subjected to full-matrix least-squares refinement on F^2 (SHELXL-97),²⁸ non-H atoms were refined anisotropically, phenyl and closed-face carborane H atoms were included with a riding model, and open-face carborane H atoms were located from difference syntheses and refined with B–H distance restraints. Restraints were also applied to the temperature factors of the light atoms and to ring planarity. Further details are given in Table 4.

Molecular Orbital Calculations. The geometry optimizations were performed by means of ab initio calculations with the Gaussian 98 program²⁹ at the Hartree–Fock and the second-order Møller–Plesset (MP2) level³⁰ with a LanL2DZ basis set, which includes Dunning and Huzinaga full double ζ for first-row atoms³¹ and Los Alamos effective core potentials including relativistic effects for the heavy atoms, plus double ζ for the rest of the elements.³² The optimizations were

- (26) Westland, A. D. *Can. Chem.* **1969**, *47*, 4135.
 (27) Alexander, R. P.; Schroeder, H. *Inorg. Chem.* **1963**, *2*, 1107.
 (28) Sheldrick, G. M. *SHELXL-97. A Program for Crystal Structure Refinement*; University of Göttingen: Göttingen, 1997.
 (29) Frisch, M. J.; Trucks, G. W.; Schlegel, H. B.; Scuseria, G. E.; Robb, M. A.; Cheeseman, J. R.; Zakrzewski, V. G.; Montgomery, J. A., Jr.; Stratmann, R. E.; Burant, J. C.; Dapprich, S.; Millam, J. M.; Daniels, A. D.; Kudin, K. N.; Strain, M. C.; Farkas, O.; Tomasi, J.; Barone, V.; Cossi, M.; Cammi, R.; Mennucci, B.; Pomelli, C.; Adamo, C.; Clifford, S.; Ochterski, J.; Petersson, G. A.; Ayala, P. Y.; Cui, Q.; Morokuma, K.; Malick, D. K.; Rabuck, A. D.; Raghavachari, K.; Foresman, J. B.; Cioslowski, J.; Ortiz, J. V.; Stefanov, B. B.; Liu, G.; Liashenko, A.; Piskorz, P.; Komaromi, I.; Gomperts, R.; Martin, R. L.; Fox, D. J.; Keith, T.; Al-Laham, M. A.; Peng, C. Y.; Nanayakkara, A.; Gonzalez, C.; Challacombe, M.; Gill, P. M. W.; Johnson, B.; Chen, W.; Wong, M. W.; Andres, J. L.; Gonzalez, C.; Head-Gordon, M.; Replogle, E. S.; Pople, J. A. *Gaussian 98*, revision A.6; Gaussian, Inc.: Pittsburgh, PA, 1998.
 (30) (a) Møller, C.; Plesset, M. S. *Phys. Rev.* **1934**, *46*, 618. (b) Binkley, J. S.; Pople, J. A. *Int. J. Quantum Chem.* **1975**, *9*, 229. (c) Binkley, J. S.; Pople, J. A.; Seeger, R. *Int. J. Quantum Chem.* **1976**, *S10*, 1. (d) Krishnan, R.; Pople, J. A. *Int. J. Quantum Chem.* **1978**, *14*, 91. (e) Krishnan, R.; Frisch, M.; Pople, J. A. *J. Chem. Phys.* **1980**, *72*, 4244.
 (31) Dunning, T. H., Jr.; Hay, P. J. In *Modern Theoretical Chemistry*; Schaefer, H. F., III, Ed.; Plenum: New York, 1976; Vol. 3, p 1.
 (32) (a) Hay, P. J.; Wadt, W. R. *J. Chem. Phys.* **1985**, *82*, 270. (b) Wadt, W. R.; Hay, P. J. *J. Chem. Phys.* **1985**, *82*, 284. (c) Hay, P. J.; Wadt, W. R. *J. Chem. Phys.* **1985**, *82*, 2299.

performed on a model cluster, $[\text{Au}_4(\text{AsH}_3)_2(\text{H}_2\text{PCH}_2\text{CH}_2\text{PH}_2)_2]^{2+}$, with C_2 symmetry, without any further restrictions except the phosphine bite angle, P–Au–P, which was kept close to the experimental value (90°). A single point calculation was run on the same model taking the experimental geometry for the cluster core ($\text{Au}_4\text{As}_2\text{P}_4$) and adding the hydrogen atoms in the appropriate positions. $[\text{AuPH}_3]_4^{2+}$ was used as a model to study the tetrahedral clusters.

The extended Hückel calculations³³ were performed using the CACAO program³⁴ with modified H_{ij} values.³⁵ The basis set for the metal atoms consisted of ns , np , and $(n - 1)d$ orbitals. The s and p orbitals were described by single Slater-type wave functions, and the d orbitals were taken as contracted linear combinations of two Slater-type wave functions. Only s and p orbitals were considered for P and As. The parameters used for Au were the following: H_{ii} (eV), ζ 6s -10.92 , 2.602; 6p -5.55 , 2.584; 5d -15.07 , 6.163, 2.794 (ζ_2), 0.6442

(33) (a) Hoffmann, R. *J. Chem. Phys.* **1963**, 39, 1397. (b) Hoffmann, R.; Lipscomb, W. N. *J. Chem. Phys.* **1962**, 36, 2179.

(34) Mealli, C.; Proserpio, D. M. *J. Chem. Educ.* **1990**, 67, 39.

(35) Ammeter, J. H.; Bürgi, H.-J.; Thibeault, J. C.; Hoffmann, R. *J. Am. Chem. Soc.* **1978**, 100, 3686.

(C_1), 0.5356 (C_2). Standard parameters were used for other atoms. Calculations were performed on models based on the crystal structures with idealized maximum symmetry, and the following distances (Å): Au–Au 2.75, Au–As 2.40, Au–P 2.36, P–H 1.40, As–H 1.50.

Luminescence Measures. Luminescence measurements were carried out using a Perkin-Elmer LS-50B luminescence spectrometer. Emission and excitation spectra were not corrected for instrumental response. Solid-state samples were packed into capillary tubes and introduced into the Perkin-Elmer variable-temperature accessory. Slit widths for excitation and emission monochromators were set at 4 nm.

Acknowledgment. This work was supported by the Spanish DGES (PB97-1010-C02-01), the Fonds der Chemischen Industrie, the CRUP and DGES (HP 1997-0041) for an Acção Integrada Luso-Espanhola. M.J.C. and L.F.V. also thank the TMR Transition Metal Clusters in Catalysis and Organic Synthesis.

IC000136Y